

Published in final edited form as:

J Am Chem Soc. 2006 September 20; 128(37): 12221–12228. doi:10.1021/ja063651p.

Stereochemical and Regiochemical Trends in the Selective Detection of Saccharides

Shan Jiang, Jorge O. Escobedo, Kyu Kwang Kim, Onur Alptürk, George K. Samoei, Sayo O. Fakayode, Isiah M. Warner, Oleksandr Rusin*, and Robert M. Strongin

Contribution from the Department of Chemistry, Louisiana State University, Baton Rouge, Louisiana 70803

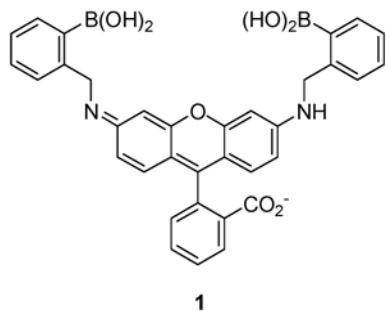
Abstract

Several discreet sugar–boronate complexes exist in solution. This is due to the complex equilibria between isomeric species of even the simplest monosaccharides. In the current investigation, we determine the regio- and stereochemical features of the various equilibrating sugar isomers that induce signal transduction in boronic acid chemosensors such as **1** as well as **2** and **3**. We present a unique example of a chemosensor (**1**) that is selective for ribose, adenosine, nucleotides, nucleosides, and congeners. As a result of this study, we are able to predict and achieve selective fluorescence and colorimetric responses to specific disaccharides as a consequence of their terminal sugar residue linkage patterns and configurations. We also find that the combined use of chemosensors exhibiting complementary reactivities may be used cooperatively to obtain enhanced selectivity for ribose and rare saccharides.

Introduction

Most arylboronic acid indicators for sugars are inherently selective for fructose or, by design, selective for glucose.¹ There is an unmet demand for chemosensors that promote the detection of other saccharides. Monitoring sugar levels is important in industry, biomedical research, and health care.

Herein we describe a boronic acid-functionalized rhodamine derivative (**1**)² which displays an unprecedented degree of colorimetric and fluorimetric selectivity for ribose and ribose derivatives. For instance, adenosine as well as nucleotides and nucleosides can be detected selectively compared to fructose, glucose, and other common saccharides. The hypothesis driving this investigation is that the characteristic regio- and stereochemical saccharide mutarotational isomer structures of specific sugars can guide indicator design.³



Results

Selective Detection of Ribose Compared to Common Monosaccharides

Ribose has been used as an anti-Hepatitis B virus (HBV) and anti-Epstein Barr virus (EBV) agent.⁴ The presence of excessive amounts of ribose has been reported in the cerebrospinal fluid (CSF, 47–146 μM) and urine (5–102 μM) of patients with ribose-5-phosphate isomerase deficiency, a disorder associated with leukoencephalopathy.^{5a} Examination of the spectral response of compound **1** to added ribose as compared to fructose, galactose, or glucose (Figure 1, parts a and b) shows that it is ribose-selective. Ribose is detected colorimetrically in this example at levels potentially relevant for diagnosing ribose-5-phosphate isomerase deficiency. The selectivity for ribose is confirmed by fluorescence spectroscopy. The emission of solutions containing **1** and ribose as well as ribose-containing compounds is generally larger compared to that of other common sugars and related biomolecules studied to date (Figure 1c).

Detection of Ribosides and Ribotides: Biomarkers of Inborn Errors of Purine Biosynthesis

Recently, a new and devastating inborn error of purine biosynthesis, AICA-ribosiduria, was discovered (Chart 1).^{5b} The child studied in this first case excreted massive levels of AICAr in her urine (280 mmol/mol creatinine). In addition, succinylaminoimidazolecarboxamide riboside (SAICAr) and succinyladenosine (S-Ado) were present at levels of 45 and 80 mmol/mol creatinine. These two latter succinylpurines are analogs of AICAr. They are also the key urinary biomarkers for the other inborn error of purine biosynthesis, adenosuccinate lyase (ADSL) deficiency. AICAr, S-Ado, and SAICAr and congeners are not present in the urine of healthy patients. In ADSL-affected children, extremely high levels, 1–10 mM in urine, 0.1 mM in cerebrospinal fluid (CSF), are present. ADSL results in mental retardation, congenital blindness, epilepsy, and dysmorphism.⁶

On the basis of the results shown in Figure 1 showing selectivity for ribose and adenosine, we hypothesize that the detection of inborn errors of purine biosynthesis biomarkers could also be feasible using **1**. Commercially available AICAr, used as a surrogate for SAICAr and S-Ado, can be readily detected in solutions containing **1** (Figure 2). Under identical experimental conditions, ATP is also detectable.

Nucleosides and nucleotides such as ATP and congeners were found at double the normal levels (ca. 1600 mmol/mL erythrocytes) in the blood of the patient with AICA-ribosiduria. Compound **1** may thus serve as a basis of future studies for a general chemical test for inborn errors of purine biosynthesis. One of the many challenges remaining involves addressing the remaining interfering signals from fructose.

Addressing Fructose Interference

Overcoming the high affinity of arylboronic acids for fructose in order to detect glucose selectively has been addressed by many researchers to date.¹ The main strategy has been to design receptors which can bind a glucose molecule selectively via two boronic acids in a bidentate fashion.⁷ Alternatively, in the current study, fructose-induced interference is eliminated by using a combination of receptors exhibiting complementary affinities and spectral properties.

Fructose-Selective Materials Used in Conjunction with **1** Heighten Selectivity for Ribose-Containing Compounds

We have previously reported an extensive study of the mechanism of chromophore formation in resorcinarene solutions.^{8a} Solutions containing millimolar concentrations of compound **2** developed micromolar levels of chromophore **3** in situ. The colored material **3** enabled saccharide detection via UV-vis and fluorescence spectroscopy. Extensive spectroscopic

studies proved that the formation of anionic sugar–boronate complexes of **3** resulted in the sugar-induced spectral changes, as boron became charged. Recently, we have used resorcinarene boronic acid (**2**) and its associated chromophoric species (**3**) produced by its oxidation for the selective detection of fructose (Figure 3).⁸

We thus hypothesize that fructose-reactive **2** (and **3**) should bind fructose and remove fructose-derived signals from solutions containing ribose-selective **1**.⁹ We indeed observe that essentially no response due to fructose (and the two other most common blood monosaccharides, galactose and glucose) occurs (Figure 4) upon adding **2** to solutions containing **1** for ribose detection.

Discussion

Chemoselective Signaling of **1** is Unique Compared to That of Other Boronic Acid Dyes

Ribose exhibits 1:1 binding to **1** according to the continuous variation method (Supporting Information). Table 1 displays the apparent binding constants (K_{eq}) corresponding to complexes of **1** with various monosaccharides. The order of affinities is ribose > allose > fructose > galactose > altrose > glucose > arabinose. The latter trend does not correlate well with the generic binding affinities involving phenylboronic acid and monosaccharides (Table 1). For instance, based on the reported similar binding constants of model arylboronate complexes of ribose and arabinose¹⁰ and the similar degree of complexation of ribose and arabinose (65% and 74%, respectively),^{3c} one would have predicted ribose to afford a spectrophotometric response similar to that of arabinose in solutions containing **1**. Since boronic acid binding alone cannot account for the colorimetric and fluorimetric selectivity observed using **1**, we thus hypothesize that secondary interactions with the rhodamine chromophore are occurring when **1** binds to specific sugars.

NMR Studies Show that **1** Binds Ribose in the Furanose Form

The ¹H NMR spectrum of a solution of **1** and ribose (0.15 M NaOD/D₂O) reveals a preference for binding ribofuranose over ribopyranose (Figure 5).¹¹ Ribofuranose possesses pairs of cis-diols for cyclic boronate formation that are more eclipsing compared to its pyranose forms.³ Ribose acetonide formation is preceded to occur at its 2,3-hydroxyls in 90% yield (Scheme 1).¹²

Ribose, Allose, Talose, Psicose, Adenosine, Nucleotides, and Nucleosides Exhibit Common Furanose Configurations

We include a total of 11 commercially available monosaccharides in our study (Figure 6). Psicose, allose, talose, and ribose are the only monosaccharides to afford spectral changes in solutions of **1** containing **2** (Figure 7). D-Psicose is a rare sugar under consideration as a direct substitute for D-fructose.¹³ Allose is a rare sugar which exhibits scavenging activity toward reactive oxygen species (ROS) and a potent inhibitory effect on the production of ROS from stimulated neutrophils.¹⁴ Additionally, allose has been used to reduce thrombus formation during postoperative period in combination with other anticlotting drugs.¹⁵ It has recently been shown to be active against ovarian cancer cell lines.¹⁶ D-Talose has shown inhibitory effects on the growth of leukemia L1210 cells.¹⁷ Tagatose (as well as fructose, vide supra) which has a relatively strong binding affinity for phenylboronic acid (comparable to that of fructose, Table 1) affords no detectable signal.

The rare ketohexose psicose exhibits a furanose form in which the 3,4-cis diols are anti to the 6-OH. Analogously, the rare aldopentoses allose and talose each possess a 2,3-cis diol moiety anti to the 1,4-substituents (shown in blue). Importantly, this is also a common feature of ribose, adenosine, and the nucleotides and nucleosides.

Simulations Show that Ribose and Congeners Can Selectively Undergo Secondary Interactions with the Fluorophore Moiety of **1**

There is precedence for secondary interactions (e.g., in the case of oligosaccharides) affording enhanced fluorescence or UV–vis signaling in boronic acid dyes.^{6a,18} Sugars possessing pentafuranose configurations with α 2,3-cis diols (for boronate ester formation) and β 1,4-substituents allow the 1,4-substituents to undergo secondary interactions with the rhodamine chromophore of **1**. Similarly, hexafuranoses exhibiting α 3,4-cis diols and β 6-OH substituents should also undergo analogous secondary interactions.

Recently, Zhu et al.,^{19a} following up on an earlier proposal by Ni et al.,^{19b} showed that in protic media (H₂O or MeOH), and particularly with relatively weaker nitrogen nucleophiles, a solvent molecule adds to boron and disrupts the B–N dative interaction between arylboronic acids containing proximal amino groups.^{19a} This results in a zwitterion wherein the nitrogen atom is protonated as the boron atom adopts sp³ hybridization and negative charge upon addition of the fourth (solvent) ligand. A hydrogen bond is concomitantly formed between the proton on nitrogen and the solvent (hydroxy or methoxy) molecule attached to boron (Figure 8).

Simulations of the boronate complexes of **1** with the furanose forms of ribose, fructose, and glucose, performed using structures that would result from solvolysis of boron, reveal how secondary interactions between the sugar moiety and the chromophore may occur selectively in the cases of ribose and its analogs. The simulations show that pentafuranoses that can exhibit an α 2,3-cis diol and β 1,4 diol configuration may have a tighter interaction with the rhodamine chromophore as compared to boronate complexes of fructose (which exhibits a well-known motif of intramolecular tridentate hydroxyl binding to boron, *vide infra*) and glucose which can bind to boron via the anomeric 1 and 2-cis hydroxyls (Figure 9). The minimized structures show that the ribofuranose complex displays the relatively best geometry for promoting direct contacts between the bound sugar moiety and the chromophore moiety of **1**. A subunit of the rhodamine chromophore moiety is shown for clarity and used in the simulations in order to simplify the calculations. The main point is that only functional groups of ribose and congeners may come within 2.2 Å of the chromophore versus >3.7 Å for other sugars studied to date. Studies aimed at evaluating the specific interactions between ribose, adenosine, ribosides, and ribotides with **1** that might involve π – π stacking, σ – π interactions, and/or charged hydrogen bonding between the sugar and the rhodamine carboxylate functionality are ongoing.

Development of **2** and **3** as Off–On Colorimetric Indicators for Sugars with Selectivity Complementary to **1**

Figure 10 shows that fluorescence emission enhancement in solutions containing **2** and **3** (using the neutral buffer sugar solution protocol described above for the studies involving **1**, where sugar in buffer is mixed with dye dissolved in DMSO) follows the expected pattern based on the affinity for phenylboronic acid according to Springsteen and Wang's¹⁰ prior studies (Table 1): fructose > arabinose > ribose > galactose > glucose. The concentration versus absorbance changes of these latter as well as other sugars, as monitored by UV–vis spectroscopy at 535 nm, is shown in Figure 11. There is scatter or no useful signal obtained from psicose, ribose, glucose, and allulose. Signaling due to the addition of tagatose, fructose, altrose, galactose, and arabinose is observed. This trend is in contrast to the responses using **1** (*vide supra*), which exhibits signal enhancement in the presence of psicose, ribose, and allulose with no detectable interference from altrose, galactose, and arabinose.

Previously, we^{8a} and others^{3b} have reported ¹³C NMR evidence for the occurrence of a distinct intramolecular tridentate fructose complex (**4**, Figure 12) in D₂O/DMSO solutions. The ability of fructose to form tridentate structures can be favored due to the well-known reactivity of the

anomeric (and adjacent) hydroxyl. Additionally, the relatively nucleophilic primary hydroxyl of β -fructofuranose is suitably positioned to also react with boron. Importantly, galactose, arabinose, and altrose, which also promote spectral responses under neutral conditions (Figure 11), possess a furanose structure similar to that of β -fructofuranose, wherein the same three binding OH groups (anomeric and adjacent as well as the primary hydroxyl) have analogous relative configurations (Figure 6). Each of these sugars may adopt furanose structures wherein the three binding hydroxyls (on the 1,2 and 5 carbons in the case of aldofuranoses and on the 2,3 and 6 carbons for ketofuranoses) are all on the same face of the furanose ring for cooperative binding to boron (Figure 6, key hydroxyls are shown in red). The saccharides that possess other configurations of these three specific hydroxyls in their furanose forms do not afford significant signal changes. Thus, each of these sugars induced signaling that is selective over psicose, ribose, glucose, and allose (Figure 11) which cannot adopt the requisite furanose structures.

Predictive Detection of Oligosaccharides via Terminal Residue Analysis

Boronic acid dyes such as **3** can be excellent chromophores for the detection of oligosaccharides.^{8a} If tridentate furanose binding to boron is indeed the origin of the selective signaling in solutions of **2** and **3**, then oligosaccharides containing residues which may form tridentate complexes with boron should also be detectable with high selectivity. In order to test this hypothesis, 12 commercially available di- and trisaccharides are studied.

Lactulose and maltulose are important disaccharides as a prebiotic oligosaccharide in milk²⁰ and as a marker of digestive disorders in infants,²¹ respectively. Of the dozen model compounds, only lactulose and maltulose can exhibit the requisite (tridentate, vide supra) configurational pattern via their terminal fructose residues (Figure 13) for signaling (Figure 14).

Conclusion

A major goal of this study was to understand the origin of the selective signal transduction mechanism in xanthene-containing boronic acids. Strong evidence is presented to show that sugars which can share the same hydroxyl configurations as ribofuranose promote signaling in solutions of **1** with high selectivity. This is the initial example of a boronic acid chemosensor which exhibits distinctive selectivity for ribose, adenosine, and derivatives as well as rare sugars such as allose and talose.

In contrast, sugars possessing configurations analogous to those found in fructofuranose can form a specific tridentate complex with **3**, resulting in selective colorimetric and fluorimetric signaling. This latter finding is successfully applied to explaining selectivity in the detection of specific disaccharides via their terminal sugar residue linkage and configurational patterns. When receptors with different optical response properties are used in tandem, interfering signals can be virtually eliminated in a relatively simple manner. The design and study of new xanthene dyes, such as **1**, **3**, and related compounds, is ongoing in our lab.

Experimental Section

UV-vis spectra were acquired on a Spectramax Plus 384 UV-vis spectrophotometer (Molecular Devices Ltd.) using a 1 cm quartz cell at 25 °C. Fluorescence emission spectra were recorded using a spectrofluorimeter SPEX Fluorolog-3 equipped with double excitation and emission monochromators, and a 400 W Xe lamp and 1 cm quartz cell at 25 °C. Altrose and allose were purchased from OMICRON Biochemicals, Inc. and Fluka, respectively. The remaining sugars as well as 4-formylphenylboronic acid and resorcinol were purchased from Sigma-Aldrich Ltd. and used without further purification. Compounds **1** and **2** were prepared according to procedures reported earlier.^{2,22}

Solutions of **2** are dissolved **1** in DMSO, heated at a gentle reflux (3 min) followed by cooling to room temperature. These solutions were mixed at room temperature with the corresponding sugars previously dissolved in phosphate buffer (pH = 7.4, 60 mM). For experiments leading to removal of fructose interference, a DMSO solution of **1** (7.2×10^{-5} M) would be added. The final solution proportions were 9:1 DMSO/buffer. The mixtures stood at room temperature for 25 min before recording UV-vis or fluorescence spectra.

Semiempirical molecular modeling analysis was performed in two steps, using MOPAC with the potential function AM1 (ChemBats3D 7.0, CambridgeSoft) to obtain an optimized geometry and then energy minimization using MM2 (ChemBats3D 7.0, CambridgeSoft). Molecular graphics images were produced using the UCSF Chimera package from the Computer Graphics Laboratory, University of California, San Francisco, CA.

Supplementary Material

Refer to Web version on PubMed Central for supplementary material.

Acknowledgements

We very gratefully acknowledge the National Institutes of Health (Grant R01 EB002044) for support of this research.

References

1. Recent reviews: (a) James TD, Shinkai S. *Top Curr Chem* 2002;218:159. (b) Wang W, Gao XM, Wang BH. *Curr Org Chem* 2002;6:1285. (c) Striegler S. *Curr Org Chem* 2003;7:81. (d) Cao HS, Heagy MD. *J Fluoresc* 2004;14:569. [PubMed: 15617264]
2. Kim KK, Escobedo JO, Rusin O, Strongin RM. *Org Lett* 2003;5:5007. [PubMed: 14682751]
3. Examples of related prior studies on saccharide conformational preferences and boronic acid complexation: (a) Norrild JC, Eggert H. *J Am Chem Soc* 1995;117:1470. (b) Norrild JC, Eggert H. *J Chem Soc, Perkin Trans 2* 1996:2583. (c) Nicholls MP, Paul PKC. *Org Biomol Chem* 2004;2:1434. [PubMed: 15136798]
4. (a) Omran H, McCarter D, StCyr J, Luederitz B. *Exp Clin Cardiol* 2004;9:117. (b) Dodd SL, Johnson CA, Fernholz K, StCyr JA. *Med Hypotheses* 2004;62:819. [PubMed: 15082114] (c) Lortet S, Zimmer HG. *Cardiovasc Res* 1989;23:702. [PubMed: 2480849] (d) Takagi Y, Nakai K, Tsuchiya T, Takeuchi T. *J Med Chem* 1996;39:1582. [PubMed: 8648597]
5. (a) Huck JHJ, Verhoeven NM, Struys EA, Salomons GS, Jakobs C, van der Knapp MS. *Am J Hum Genet* 2004;74:745. [PubMed: 14988808] (b) Marie S, Heron B, Bitoun P, Timmerman T, Van den Berghe G, Vincent MF. *Am J Hum Genet* 2004;74:1276. [PubMed: 15114530]
6. Jaeken J, Van den Berghe G. *Lancet* 1984;1058.
7. Shiomi Y, Saisho M, Tsukagoshi K, Shinkai S. *J Chem Soc, Perkin Trans 1* 1993:2111.
8. (a) He M, Johnson RJ, Escobedo JO, Beck PA, Kim KK, StLuce NN, Davis CJ, Lewis PT, Fronczek FR, Melancon BJ, Mrse AA, Treleaven WD, Strongin RM. *J Am Chem Soc* 2002;124:5000. [PubMed: 11982364] (b) Rusin O, Alpturk O, He M, Escobedo JO, Jiang S, Dawan F, Lian K, McCarroll ME, Warner IM, Strongin RM. *J Fluoresc* 2004;14:611. [PubMed: 15617268]
9. (a) Wu A, Isaacs L. *J Am Chem Soc* 2003;125:4831. [PubMed: 12696902] (b) Mukhopadhyay P, Wu A, Isaacs L. *J Org Chem* 2004;69:6157. [PubMed: 15357573] (c) Wu A, Mukhopadhyay P, Chakraborty A, Fettinger JC, Isaacs L. *J Am Chem Soc* 2004;126:10035. [PubMed: 15303878]
10. Springsteen G, Wang B. *Tetrahedron* 2002;58:5291.
11. The ^1H NMR assignments for D-ribose are based on the ones reported by: Benesi AJ, Falzone CJ, Banerjee S, Farber GK. *Carbohydr Res* 1994;258:27.
12. Cho JH, Bernard DL, Sidwell RW, Kern ER, Chu CK. *J Med Chem* 2006;49:1140. [PubMed: 16451078]
13. Matsuo T, Suzuki H, Hashiguchi M, Izumori K. *J Nutr Sci Vitaminol* 2002;48:77. [PubMed: 12026195]

14. Murata A, Sekiya K, Watanabe Y, Yamaguchi F, Hatano N, Izumori K, Tokuda M. *J Biosci Bioeng* 2003;96:89. [PubMed: 16233490]
15. Austin WC, Humoller FL. *J Am Chem Soc* 1934;56:1152.
16. Sui L, Dong YY, Watanabe Y, Yamaguchi F, Hatano N, Izumori K, Tokuda M. *Anticancer Res* 2005;25:2639. [PubMed: 16080505]
17. Lerner LM, Mennitt G. *Carbohydr Res* 1994;259:191.
18. Nagai Y, Kobayashi K, Toi H, Aoyama Y. *Bull Chem Soc Jpn* 1993;66:2965.
19. (a) Zhu L, Shabbir SH, Gray M, Lynch VM, Sorey S, Anslyn EV. *J Am Chem Soc* 2006;128:1222. [PubMed: 16433539] (b) Ni W, Kaur G, Springsteen G, Wang B, Franzen S. *Bioorg Chem* 2004;32:571. [PubMed: 15530997]
20. Rudolfova J, Curda L. *Chem Listy* 2005;99:168.
21. Morales V, Olano A, Corzo N. *J Agric Food Chem* 2004;52:6732. [PubMed: 15506809]
22. (a) Lewis PT, Davis CJ, Saraiva M, Treleaven WD, McCarley TD, Strongin RM. *J Org Chem* 1997;62:6110. (b) Davis CJ, Lewis PT, McCarroll ME, Read MW, Cueto R, Strongin RM. *Org Lett* 1999;1:331. [PubMed: 10905872]

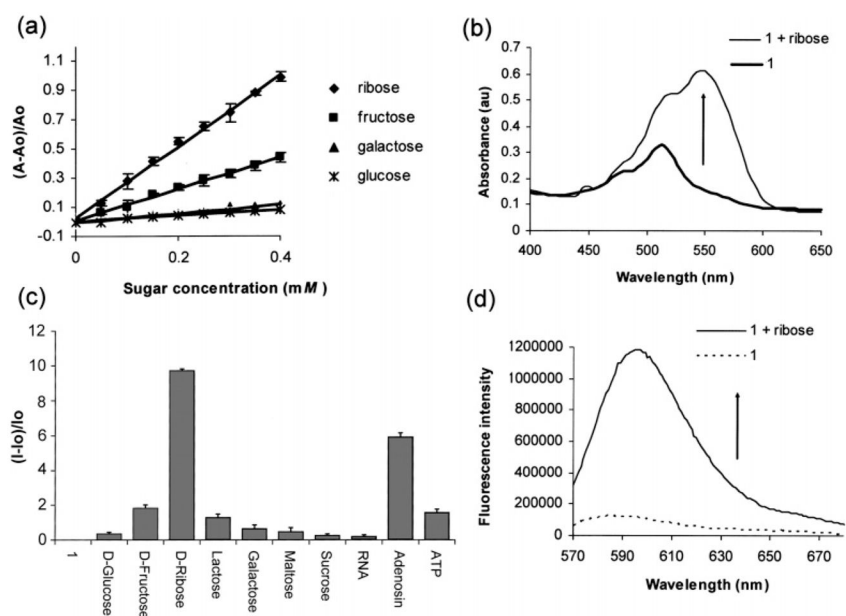


Figure 1.

(a) Relative absorbance changes vs concentration of various monosaccharides in phosphate buffer (0.1 mL, 60 mM, pH 7.4) added to **1** (7.2×10^{-5} M) in DMSO (0.9 mL) and monitored at 560 nm. (b) The UV-vis spectra of a solution of **1** (7.2×10^{-5} M) alone and **1** with added ribose (4×10^{-4} M). (c) Relative fluorescence emission spectra at 597 nm of **1** (4×10^{-9} M) and saccharides and saccharide-containing molecules (1.85×10^{-3} M) in 9:1 DMSO/phosphate buffer (0.05 M, pH 7.4) excited at 565 nm. (d) Fluorescence emission spectra of a solution of **1** (4×10^{-9} M) and **1** with added ribose (1.85×10^{-3} M) in 9:1 DMSO/phosphate buffer (0.05 M, pH 7.4) excited at 565 nm.

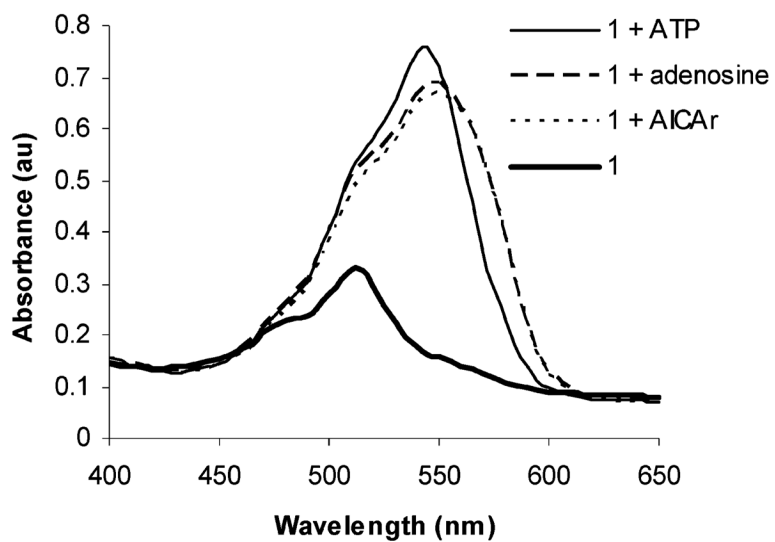
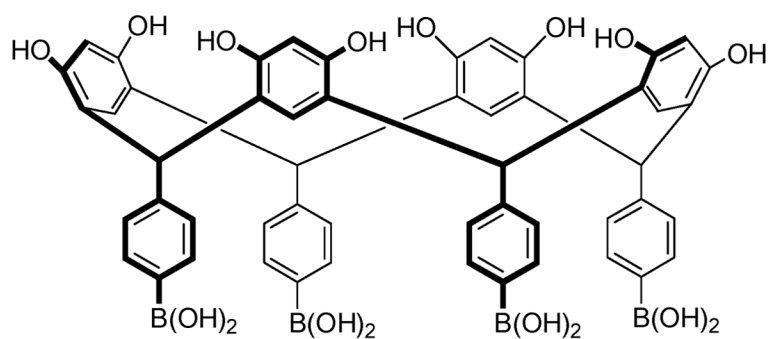
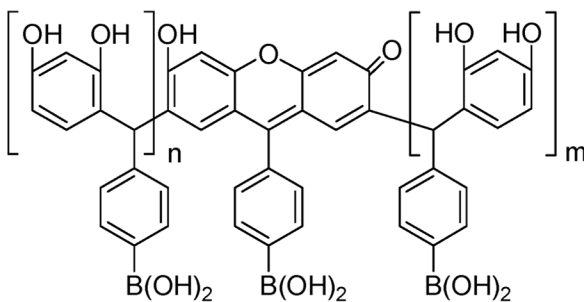


Figure 2. UV-vis spectra of solutions containing **1** (7.2×10^{-5} M) in 9:1 DMSO/phosphate buffer (0.06 M, pH 7.4) and **1** in the presence of 4×10^{-4} M solutions of ATP, adenosine, and AICAr.

**2**

3 $n = 0, 1, 2, \text{etc}$
 $m = 0, 1, 2, \text{etc}$

Figure 3. Structures of the resorcinarene boronic acid **2** and its chromophoric products (**3**) formed in situ.

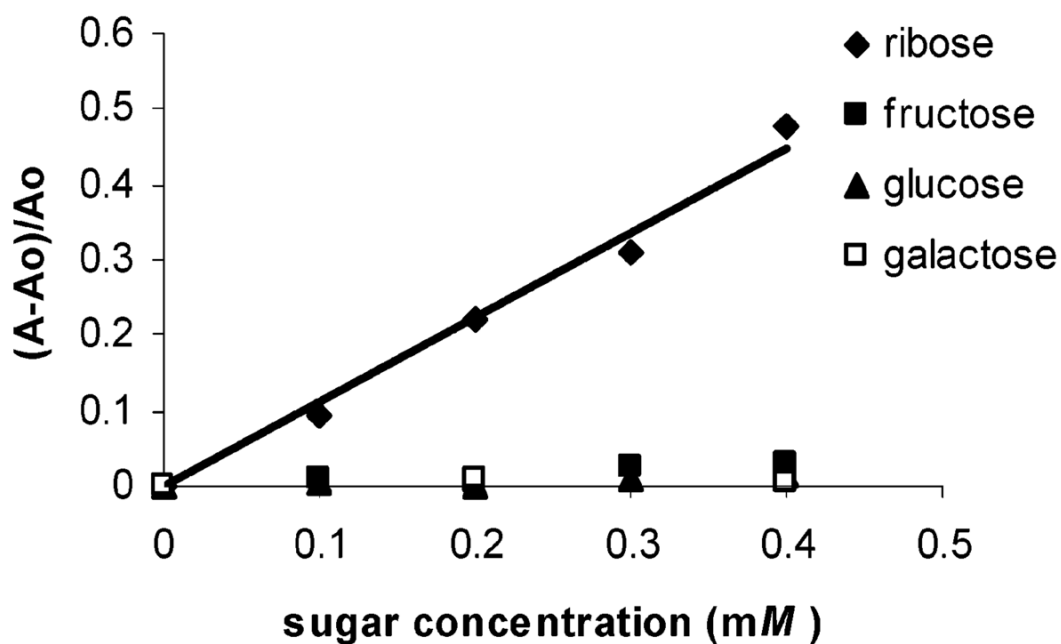


Figure 4. Relative absorbance changes vs concentration of ribose, fructose, galactose, and glucose in solutions comprised of phosphate buffer (0.1 mL, 60 mM, pH = 7.4) added to **1** (0.07 mM) in DMSO (0.9 mL) and **2** (1.9 mM) monitored at 560 nm. A comparison to Figure 1a shows that the use of **1** combined with **2** removes significant fructose interference under these conditions.

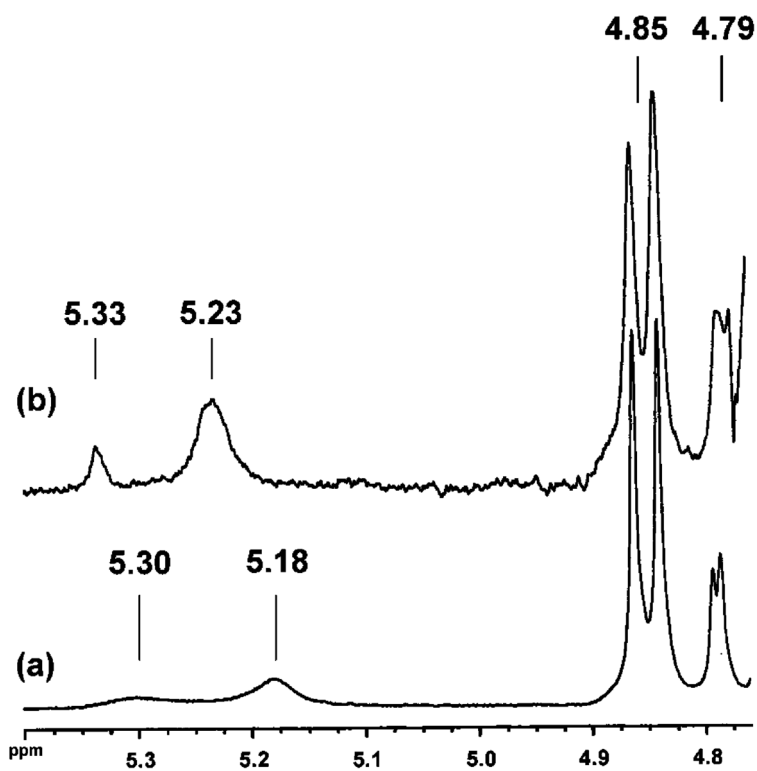


Figure 5. Expansion of the ¹H NMR spectra of solutions of (a) D-ribose and (b) a mixture of **1** and D-ribose (0.15 M NaOD/D₂O). The resonances shown correspond to the anomeric protons of each of the four cyclic forms. The assignments are δ (ppm): 5.30 (α -ribofuranose), 5.18 (β -ribofuranose), 4.85 (β -ribofuranose), and 4.79 (α -ribofuranose). Upon the addition of **1** only the resonances corresponding to the ribofuranoses exhibit a downfield shift. This is expected as a result of cyclic boronate formation with ribofuranose (ref 3c).

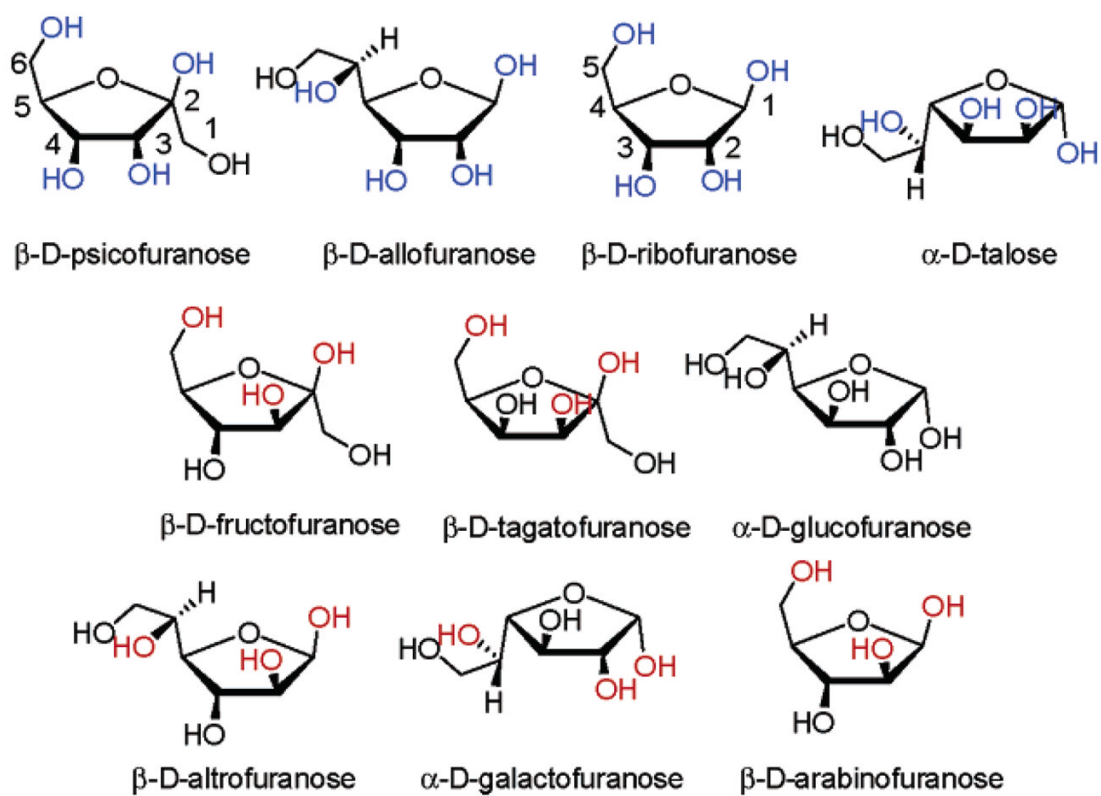


Figure 6. Structures of 11 monosaccharides in their furanose forms. Compound **1** is selective for sugars with hydroxyls shown in blue. Compound **3** is selective for sugars with hydroxyls shown in red.

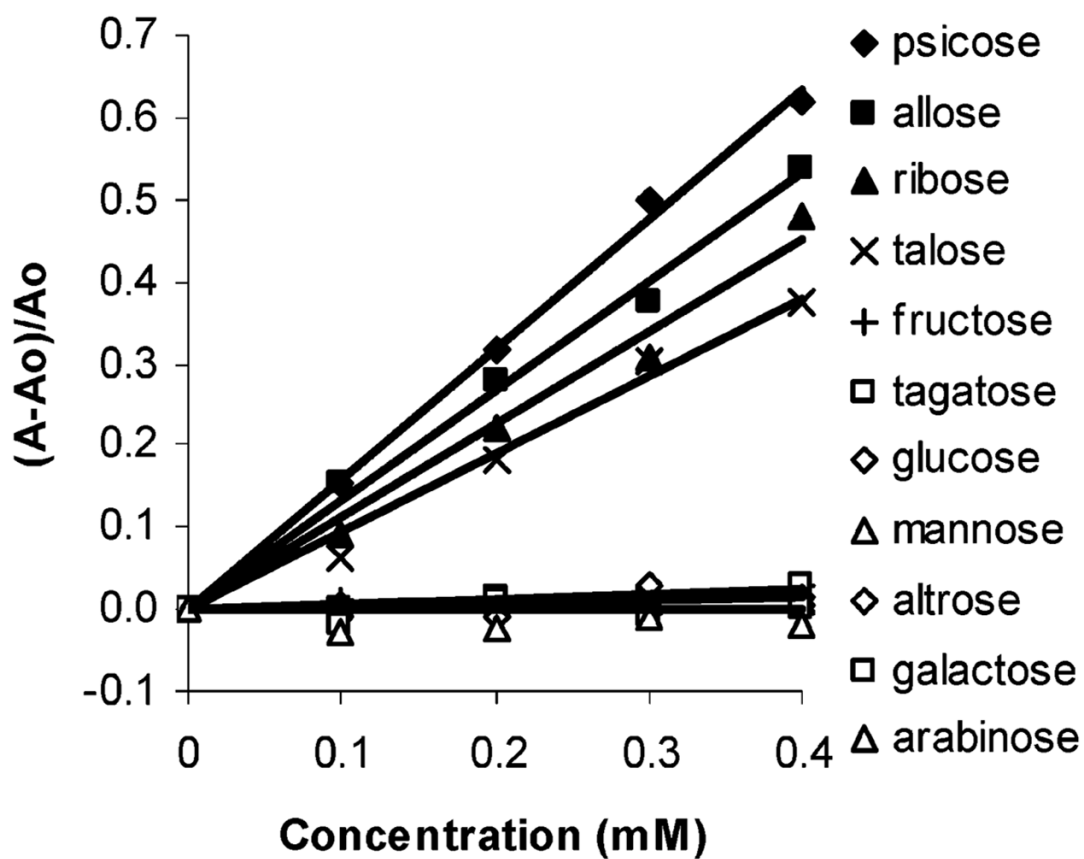


Figure 7.

Plots of relative absorbance changes vs concentration of 11 monosaccharides in solutions comprised of phosphate buffer (0.1 mL, 60 mM, pH = 7.4) added to **1** (0.07 mM) in DMSO (0.9 mL) and **2** (1.9 mM) monitored at 560 nm.

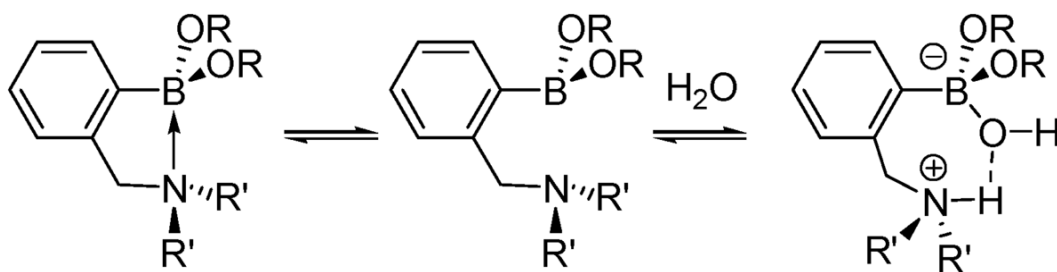


Figure 8.
Effect of solvation on the B–N bond in *o*-(*N,N*-dialkylamino-methyl)phenylboronic esters
(adapted from ref ^{19a}).

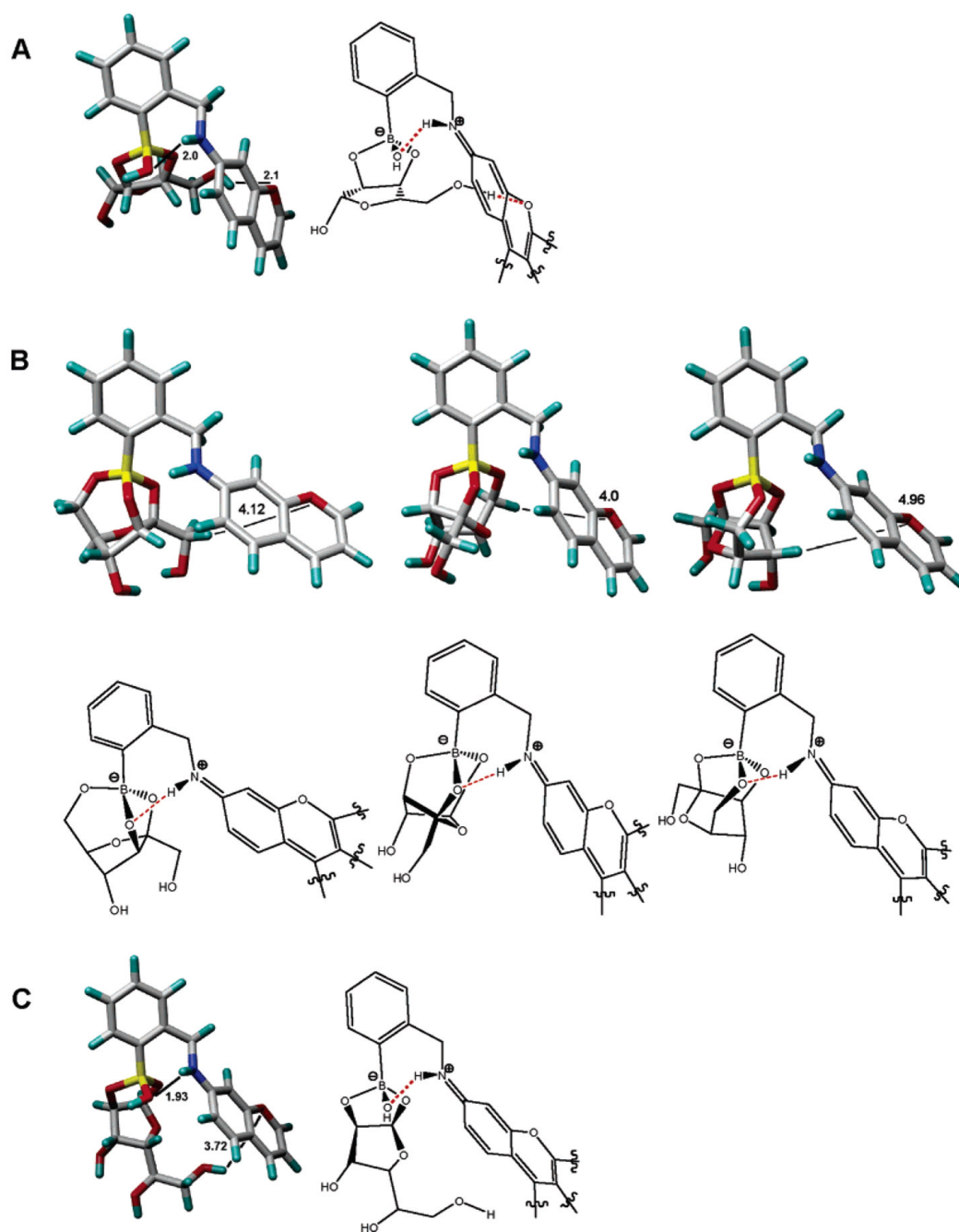


Figure 9.

Energy-minimized structures of boronates derived from **1** and ribofuranose (“endo” isomer, structure A), fructofuranose (three rotamers, structures B), and glucofuranose (“exo” isomer, structure C; the complementary conformers of the ribo- and glucofuranose boronates are included in the Supporting Information). A subunit of the rhodamine chromophore moiety is shown for clarity and used in the simulations in order to simplify the calculations. The above-calculated structures show that the ribofuranose complex exhibits the relatively best geometry for promoting direct contacts between the bound sugar moiety and the chromophore moiety of **1**. Studies aimed at evaluating the specific interactions between ribose, adenosine, ribosides,

and ribotides with **1** that might involve π - π stacking, σ - π interactions, and/or charged hydrogen bonding between the sugar and the rhodamine carboxylate functionality are ongoing.

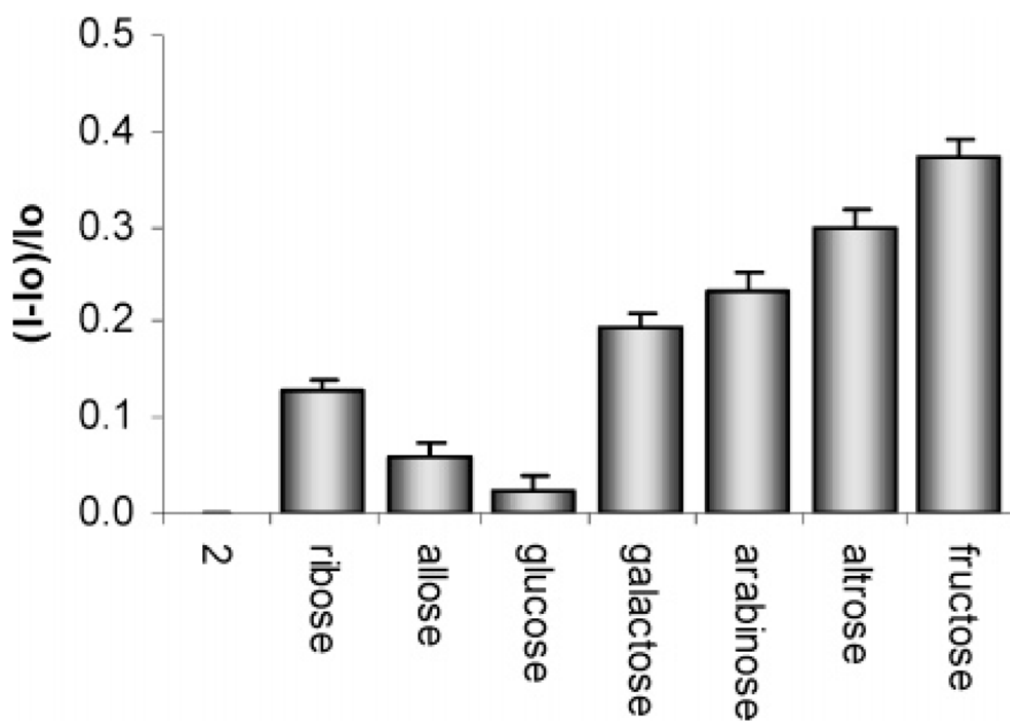


Figure 10. Relative fluorescence emission spectra at 574 nm of **2** (5.75×10^{-5} M) and monosaccharides (1.85×10^{-3} M) in 9:1 DMSO/phosphate buffer (0.05 M, pH 7.4) excited at 550 nm.

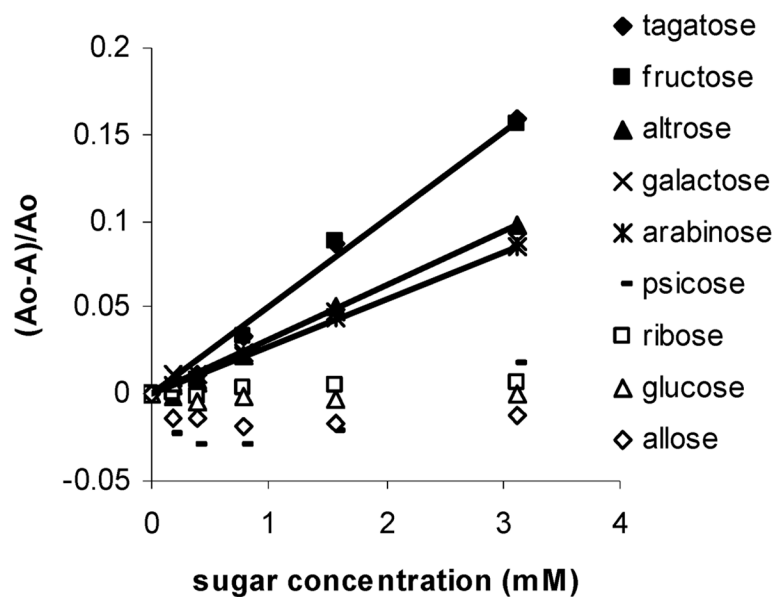


Figure 11. Relative absorbance changes vs the concentration of various monosaccharides in phosphate buffer (0.1 mL, 60 mM, pH = 7.4) added to **2** in DMSO (3.4 mM, 0.9 mL) at 535 nm.

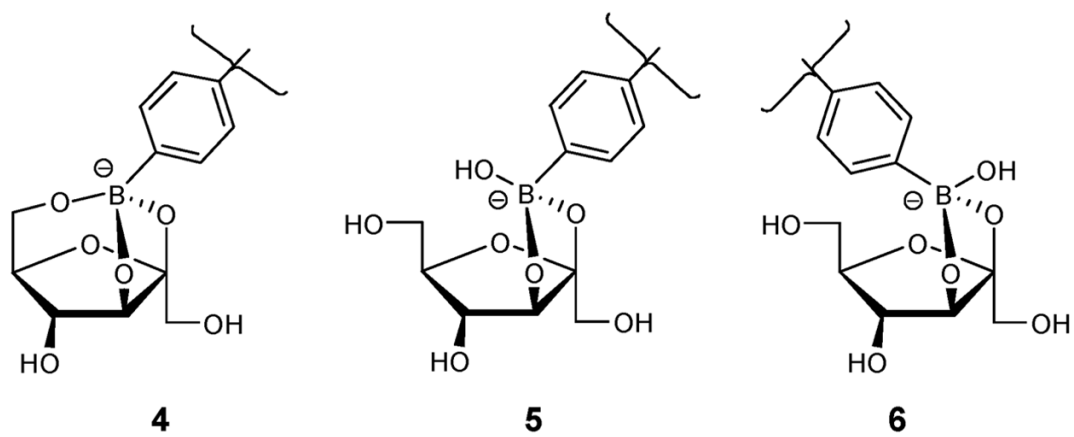


Figure 12.
Anionic fructofuranose-boronate ester structures.

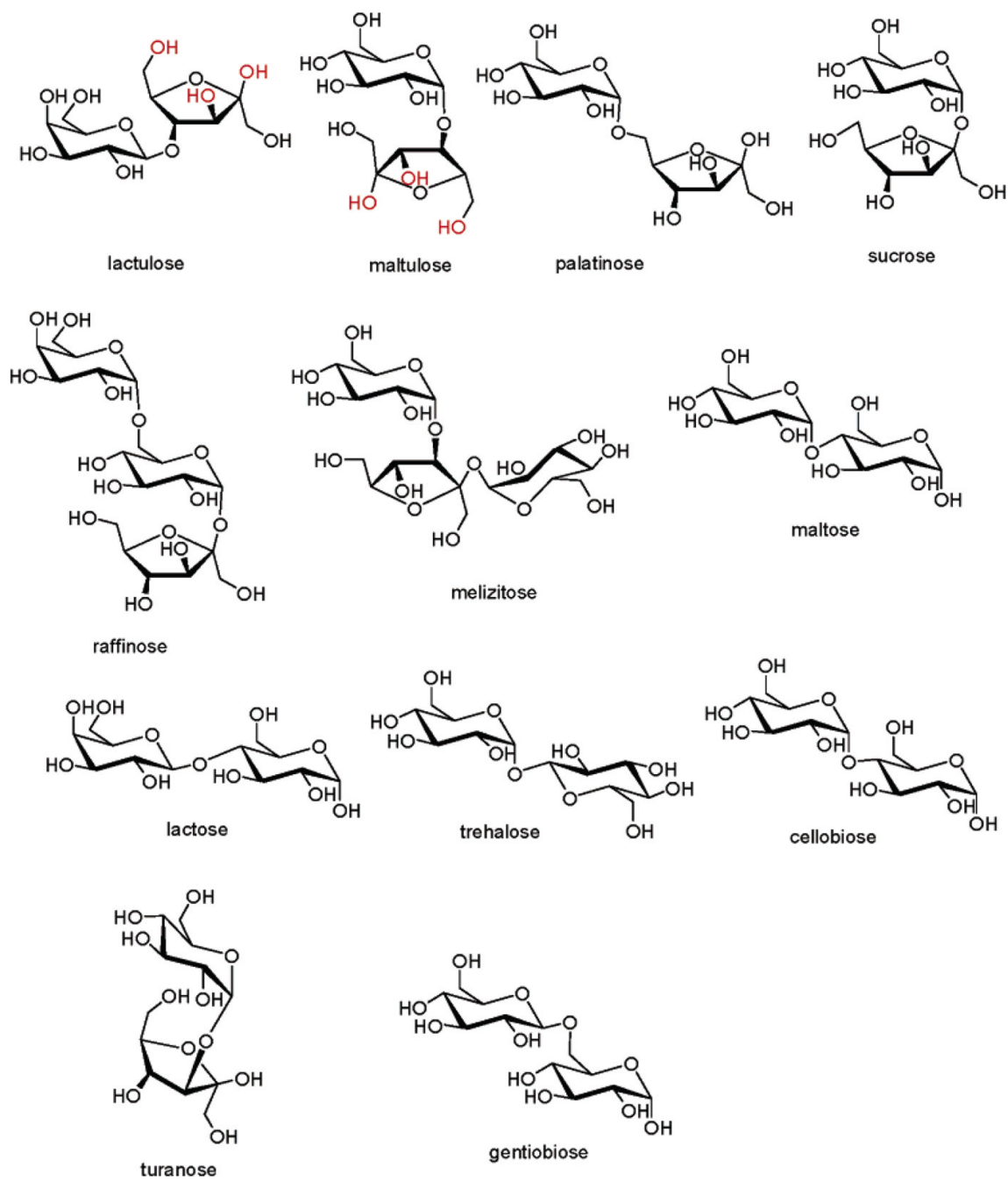


Figure 13.
Di- and trisaccharides studied.

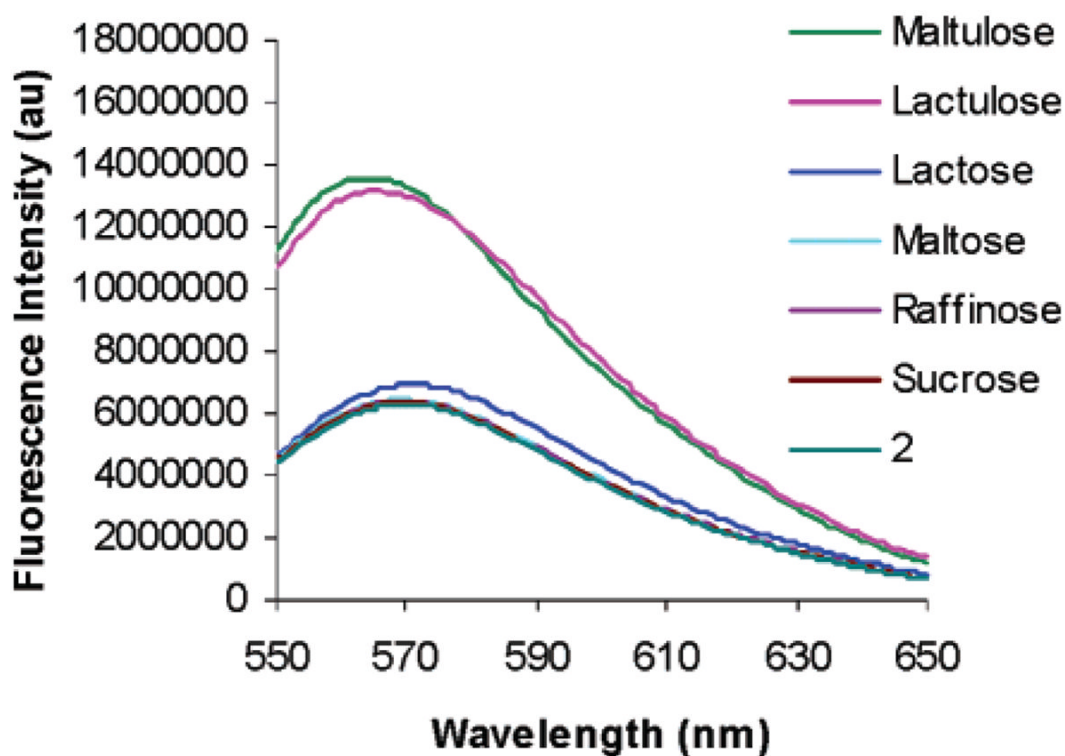
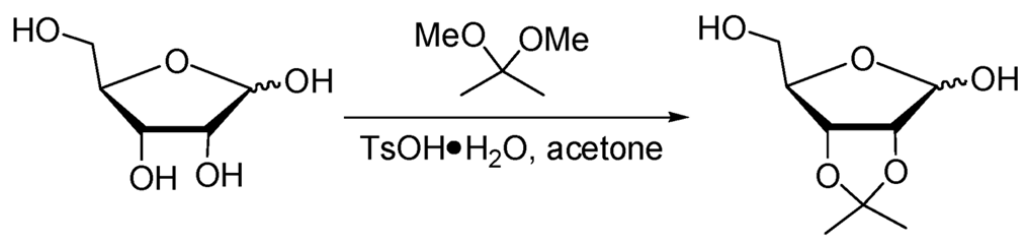


Figure 14.

Fluorescence emission spectra of a solution of **2** (1×10^{-3} M) and **2** with added di- and trisaccharides (1.85×10^{-3} M), all in 9:1 DMSO/phosphate buffer (0.05 M, pH 7.4) excited at 535 nm. This result shows the selectivity for lactulose and maltulose. The other di- and trisaccharides tested afford no detectable signal. Only lactulose and maltulose can adapt the proper terminal residue configurational preference (Figure 13). The selectivity is confirmed by UV-vis spectroscopy (Supporting Information).



Scheme 1.
Formation of Ribose Acetonide via Selective Reaction of the 2,3-Hydroxyls in 90% Yield (Ref 12)

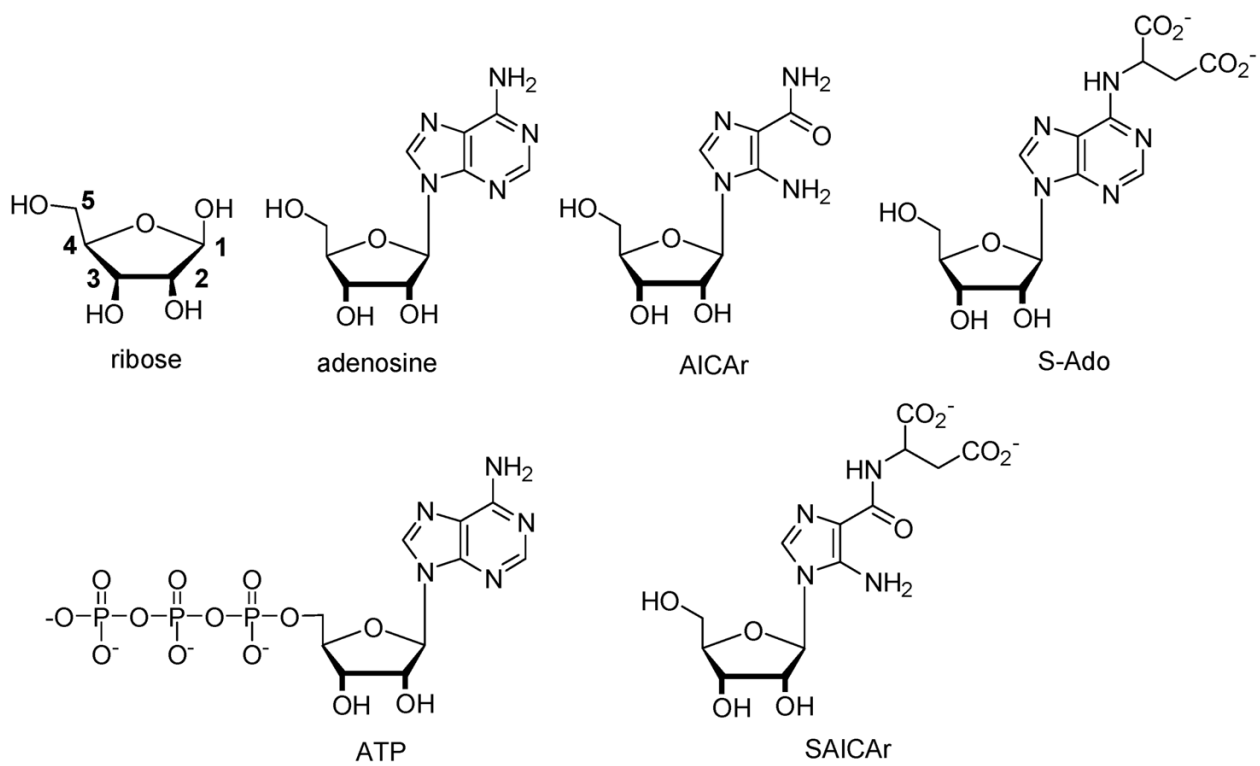


Chart 1.

Table 1

Apparent Binding Constants (K_{eq}) of the Complexes of Various Monosaccharides and Compound **1** (7.2×10^{-5} M in 9:1 DMSO/Phosphate Buffer 60 mM, pH 7.4)^a

saccharide	K_{eq} (M^{-1})	
	calcd values for 1	literature values for phenylboronic acid ^b
ribose	2400	24
allose	1500	
fructose	1100	160
galactose	310	15
altrose	270	
glucose	200	4.6
arabinose	120	25

^a Values are the average of three runs rounded to two significant figures. The binding constants taken from the literature were generated in aqueous solution, while those from the current study were from DMSO/buffer solution. The absolute values are thus not directly comparable.

^b See ref 10.